journal

J. Am. Ceram. Soc., 89 [1] 13–19 (2006)
DOI: 10.1111/j.1551-2916.2005.00657.x

Temperature-Induced Structural Modifications Between Alkali Borate Glasses and Melts

L. Cormier,*,†,‡ O. Majérus,‡,§ D. R. Neuville,¶ and G. Calas*,‡

‡Institut de Minéralogie et de Physique des Milieux Condensés, CNRS UMR 7590, Universités Paris 6 et Paris 7, Institut de Physique du Globe, 75005 Paris, France

¶Physique des Minéraux et des Magmas, CNRS UMR 7047, Institut de Physique du Globe, 75005 Paris, France

High-temperature neutron diffraction and Raman spectra have been obtained on M_2O–$2B_2O_3$ (M = Li, Na, K) glasses and melts. Both techniques indicate a coordination change of boron atoms: the tetrahedral boron sites present in the glasses are converted into triangular boron sites. These changes of the borate network yield modifications of the alkali environment, as assessed for Li using the isotopic substitution technique. We observe that Li atoms are in a charge-compensating position in the glass and in a modifying position in the liquid. These structural modifications have important implications toward understanding the physical properties of borate melts.

I. Introduction

Structural changes above the glass transition temperature (T_g) are expected to have drastic consequences on the transport (viscosity, diffusion) and thermodynamic (molar expansivity, compressibility, heat capacity) properties of melts. An adequate understanding of the temperature dependence of melt properties requires information on both structure and dynamics. For temperatures above T_g, the melt or the supercooled melt is able to reach its equilibrium state through continuous configurational changes that contribute to thermodynamic properties. These structural changes can be related to the non-Arrhenian temperatures dependence of viscosity within the framework of the configurational entropy theory.[1]

Alkali borate systems are attractive materials from a fundamental point of view and for technological interest. Indeed, borate glasses are easily quenched for a wide range of composition, and continuous variations of their structure, properties, and dynamics are observed with the alkali content.[2] Addition of alkali oxide to pure B_2O_3 causes a progressive change of the boron atom coordination number (CN), from 3 ($^{[3]}$B) to 4 ($^{[4]}$B), and results in the formation of various cyclic units (diborate, triborate, tetraborate groups etc.) that contain both $^{[3]}$B and $^{[4]}$B, and whose relative concentrations depend on the alkali content.[2–5] The effect of modifier content on the glass structure has been particularly investigated by NMR[3,4] and vibrational works.[2,5] These studies have evidenced the formation of $^{[4]}$B up to about 35 mol% alkali oxide without significant formation of non-bridging oxygen (NBO). At higher alkali content, the proportion of BO_4 units, $N4 = {}^{[4]}B/({}^{[4]}B+{}^{[3]}B)$, decreases while NBOs are formed, which yield a depolymerization of the borate network. The proportion of $^{[4]}$B is also affected by the nature of the alkali, and the environment around alkalis has been elucidated in particular by far-infrared spectroscopic studies, which show the presence of two distinct components in the vibrating modes of alkali sites.[6,7] These two contributions may be associated with a charge-compensating role around the BO_4 units and a modifying role near NBOs, according to Molecular Dynamics simulation.[8] However, this interpretation may be questioned, and the two far-IR absorption bands have been alternatively interpreted as two different vibrational modes arising from only one distribution of alkali sites,[9] or two types of environments corresponding to singly and doubly occupied anionic sites.[10]

Only recently has the structural evolution of borate glasses with temperature been investigated. In pure B_2O_3 melt, temperature-induced structural changes have been described as a modification of ring statistics, with the gradual opening of the boroxol rings above the glass transition temperature, T_g.[11–13] In alkali borate glasses, the decrease of the number of $^{[4]}$B with temperature increasing above T_g has been observed with *in situ* high-temperature ^{11}B NMR,[14] Raman spectroscopy,[15,16] and X-ray and neutron diffraction.[17–20] However, the lack of a quantitative evaluation of changes observed in experimental data precludes a clear structural interpretation of the glass to liquid transition in alkali borates. As explained above, the topic of surroundings of alkalis in borate glasses is still controversial, and high-temperature measurements should provide valuable information as the structural role of the cation should be modified during the boron coordination change.

In this paper, we present a study of the structural modifications between the glassy and liquid state in M_2O–$2B_2O_3$ systems, with M = Li, Na, and K, by using neutron diffraction and Raman spectroscopy. The neutron total structure factors and correlation functions have been obtained from room temperature up to 1200 K, and present important variations at local and medium range distances. The diborate composition has been chosen as it corresponds to the largest proportion of boron in fourfold coordination in this binary system. The proportion of $^{[4]}$B to $^{[3]}$B was experimentally observed by a careful analysis of the neutron total correlation function and by the deconvolution of a high-intensity band in Raman spectra. The two methods agree with a partial conversion of the BO_4 units in the glass to BO_3 units in the liquid. This species exchange may account for the main part of the configurational entropy of these systems, and may be the fundamental mechanism for the liquid to relax and flow. By using Li isotopic substitution, we extracted the well-defined Li-centered correlation functions for the glass and for the melt. A shortening of the mean Li–O distance between glassy and liquid states indicates an increasing modifying role of Li in the borate melt. A comprehensive picture of the structural changes between Li diborate glasses and melts is proposed and placed in relation with transport properties in these melts.

II. Experimental Procedure

(1) Materials

Glasses of composition M_2O–$2B_2O_3$ with M = Li, Na, or K were prepared from dried reagent grade powders of boron oxide

D. Green—contributing editor

Manuscript No. 20396. Received April 10, 2005; approved June 16, 2005.
Presented at the 107th Annual Meeting of The American Ceramic Society, Baltimore, April 12, 2005.
*Member, American Ceramic Society.
†Author to whom correspondence should be addressed. e-mail: cormier@lmcp.jussieu.fr
§Present address: Laboratoire de Chimie Appliquée de l'Etat Solide, Ecole Nationale Supérieure de Chimie de Paris, 11 rue Pierre et Marie Curie, 75231 Paris Cedex 05, France.

and alkali carbonate (Li_2CO_3, Na_2CO_3, K_2CO_3). Boron was isotopically enriched in ^{11}B (99.62%) to avoid the high neutron absorption cross-section of the ^{10}B isotope. For the Li_2O–$2B_2O_3$ composition, two glasses were synthesized using $^6Li_2CO_3$ (95.7% ^6Li) for the first glass and $^7Li_2CO_3$ (99.94% ^7Li) for the second glass. We use the notation NB2 and KB2 for the glasses containing Na and K, respectively, and 7LB2 and 6LB2 for the ^7Li-enriched glass and the ^6Li-enriched glasses, respectively. The starting powders were melted for 1 h at 900°C, quenched by immersion of the bottom of the Pt crucible in water, and then crushed and remelted for 15 min at 1050°C and quenched again, to ensure glass homogeneity. The LB2 glasses, whose melt temperature is higher (917°C) than NB2 and KB2, were melted for 20 min at 1020°C twice. Analyses of the chemical compositions are reported in Table I, along with the glass transition temperatures. The densities of the glasses were measured by the Archimedes method, with toluene as the liquid reference, and compared well with previous data.[21]

(2) Neutron Diffraction Experiments and Data Analysis

Neutron diffraction experiments were carried out on the 7C2 diffractometer at the Orphée reactor of the Laboratoire Léon Brillouin (Orsay, France). This instrument uses hot neutrons of wavelength 0.718 Å, preventing access to a Q-range of 0.5–16 $Å^{-1}$. Glasses were powdered just before the measurement in order to present hydration, and set in a cylindrical vanadium cell at the center of a cylindrical vanadium furnace. Measurements were performed on the glass and melt, at room temperature and 1273 K, respectively. Complementary measurements of the scattering from the empty cans in the furnace at 300 and 1273 K, from the empty furnace at 300 K, and from the background were performed for use in the data analysis procedure. The use of a V cell, which mainly yields an incoherent scattering, is essential compared with a Pt cell, which may be used but may lead to difficulty in removing Bragg peaks,[22] which may preclude the observation of small structural changes as in previous studies.[18] The 7LB2 and 6LB2 glasses were also investigated at room temperature using the SANDALS instrument at the ISIS spallation neutron source (Rutherford Appleton Laboratory, Chilton, U.K.), to provide a correlation function with a high real space resolution ($0.1 < Q < 50$ $Å^{-1}$). The data were corrected as described previously.[19,20] The data reduction yields the total structure factor, $F(Q)$, which is the distinct scattering term of the total neutron cross-section. The total radial distribution function, $T(r)$, is obtained by Fourier transformation of $F(Q)$ and corresponds to the neutron-weighted sum of all the partial pair distribution functions $g_{\alpha\beta}(r)$ (the notations are those used in Majérus *et al.*[20]).

The isotopic substitution technique[23] consists of subtraction of the total structure factors of the 6LB2 and 7LB2 samples, which allows cancellation of identical terms (B–B, B–O, and O–O) and yields only a weighted sum of the Li-centered partial structure factors (Li–O, Li–B, and Li–Li). By Fourier transforming this differential structure factor, $\Delta_{Li}(Q)$, one obtains a correlation function, $T_{Li}(r)$, which is the sum of all the Li-centered partial correlation functions.

Table I. Molar Compositions Measured by Chemical Analysis, Glass Transition (T_g) and Melt Temperatures (T_m), and Atomic Number Density for the Alkali Borate Glasses

	7-LB2	6-LB2	NB2	KB2
M_2O (mol%)	37.07	38.56	35.8	34.8
B_2O_3 (mol%)	62.93	61.44	64.2	65.2
T_g (K)†	773	773	752	705
T_m (K)	1190	1190	1015	1088
$\sigma \pm 0.001$ atoms $Å^{-1}$	0.104	0.104	0.091	0.077

†Glass transition temperatures are determined by ATD.

(3) Raman Spectroscopy

Raman spectra were recorded using a T64000 Jobin–Yvon confocal micro-Raman spectrometer equipped with a charge-coupled device (CCD) detector (Jobin Yvon, NJ) for the LB2 sample. The emission line at 514.532 nm of a coherent 70–C5 Ar+ laser was used for sample excitation, with an incident power of about 2.8 W. This excitation and CCD system results in a signal-to-noise ratio of 80/1. The integration time was 30 s. With our triple spectrometer, we can collect spectra over a wide frequency range (10–1800 cm^{-1}). All reported spectra are unpolarized. High-temperature measurements were obtained with a home-made heating unit, and the spectra were corrected for temperature effects.[24,25] The corrected Raman intensities were normalized to the data point of the greatest absolute intensity. Spectra were recorded between room temperature and up to the liquid state at 1350 K, but crystallization (spectra not shown) occurred between 1280 and 1359 K.

III. Results

(1) Total Neutron Functions

The total structure factors at room and high temperature are shown in Fig. 1. The high Q-range ($Q > 5$ $Å^{-1}$), which can be attributed to the short-range order, presents a dampening of the oscillations at high temperature because of both static and thermal disorder. The oscillations at the low-Q region are related to medium-range correlations (4–20 Å), involving preferred arrangements between borate units and/or alkali ions. The first peak is shifted toward lower Q values for Li (1.53 $Å^{-1}$), Na (1.40 $Å^{-1}$), and K (1.26 $Å^{-1}$), which implies structural organization with a larger correlation distance with increasing cation size. At high temperature, the intensity of this peak decreases without any significant shift in position, except for KB2, where the peak is shifted at 1.21 $Å^{-1}$, indicating an expansion of the medium-range structural correlations.

In real space, the total correlation functions (Fig. 2) are characterized by two strong contributions at 1.4 and ~2.4 Å. The first peak is a result of the B–O pairs, and the second is mainly a result of O–O pairs and small contributions from B–B, Na–O, and K–O pairs. The Li–O pair is clearly observed around 2 Å as

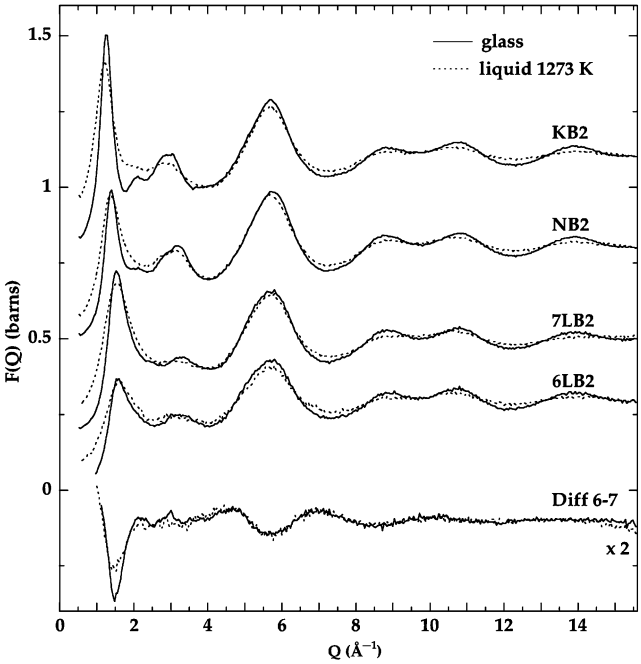

Fig. 1. Total structure factor for the KB2, NB2, 7LB2, and 6LB2 glasses (plain curves) and liquids (dashed curves) and corresponding first difference structure factor between the 6LB2 and 7LB2 samples (multiplied by 2 for clarity).

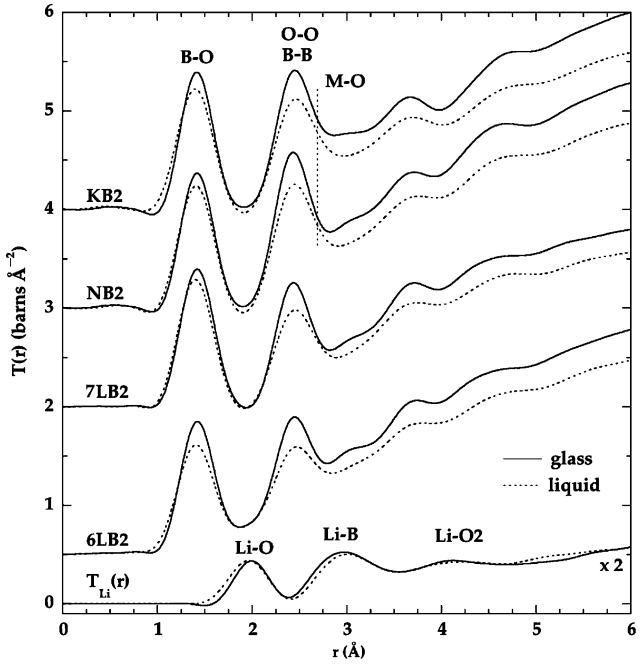

Fig. 2. Total correlation functions for the KB2, NB2, 7LB2, and 6LB2 glasses (plain curves) and liquids (dashed curves), obtained by Fourier transforms (FT) of the $F(Q)$ on the Q range 0.6–15.56 $Å^{-1}$ modified by a Lörch function. Li-centered functions, $T_{Li}(r)$, for the LB2 glass (plain lower curve) and liquid (dashed lower curve), obtained by FT of the first-difference structure factor on the Q range 1.0–14.32 $Å^{-1}$ modified by a Lörch function (multiplied by 2 for clarity). The oscillations at low r were removed by an inverse FT procedure.

a difference in intensity because of the different neutron scattering length of ^{6}Li and ^{7}Li isotopes. Contributions at higher r-values are mainly related to the borate network. With increasing temperatures, the B–O contributions shift from 1.425 to 1.410 Å and correspond to a change in the mean boron coordination. It should be emphasized that this change in the first B–O peak appears only above the glass transition temperature. The peaks at medium range distance (2.2–5 Å) are reduced in intensity, and the O–O peak at 2.6 Å is slightly shifted by 0.01 Å on the high r side.

Quantitative information has been extracted from fits of the first B–O peak using two Gaussian functions at room temperature (modeling the BO_3 and BO_4 units separately) and only one Gaussian function in the liquid because of the thermal broadening that reduces the resolution (Table II). The accuracy of the parameters obtained by such fitting (mean B–O distance, R, Debye–Waller factor, σ, and CN) has been carefully evaluated previously.[19]

The B–O distances determined in the glasses agree with those expected for the BO_3 and BO_4 units.[11,12] The average distance determined in the liquid state decreases by about 0.01 Å compared with the mean distance in the glassy state. This shortening of the B–O distance results from two effects: the decrease of the BO_4/BO_3 ratio, which reduces the mean B–O distance, and the thermal expansion of the B–O bond. However, the latter effect is negligible because the mean linear expansion coefficients for the $^{[3]}$B–O and the $^{[4]}$B–O bond (4×10^{-6} and 5.3×10^{-6} K^{-1}, respectively[26]) imply a B–O bond length increased by 0.004 and 0.005 Å at 1273 K, which is far below the experimental resolution. Therefore, the variation of the B–O distance is dominated by a boron coordination decrease.

The proportion of $^{[4]}$B, N4, can been assessed using the CNs or the average distances independently.[18] The fractions of $^{[4]}$B determined from the neutron diffraction data are in good agreement with NMR determinations in the glassy state.[3] We observe that the proportion of N4 decreases with the cation size in the glasses. This is consistent with NMR and Raman studies that found a trend for smaller alkali cations to favor borate groups containing BO_4 tetrahedra.[2] On the contrary, in the liquid, no clear trend as a function of the alkali type could be observed, given the precision of the data.

(2) First Difference Neutron Functions for Li

The environment of alkalis is difficult to investigate in the total correlation function because of the overlapping of all the pairs. For instance, the first Na–O or K–O contributions are merged with the strong first O–O and B–O contributions at 2.4 Å. Therefore, recourse to the isotopic substitution technique is essential to gain an insight in the alkali environment, and only Li has suitable isotopes for such a method. The first difference structure factors, $\Delta_{Li}(Q)$, and correlation functions, $T_{Li}(r)$, have been obtained by subtracting the neutron data for the 6LB2 and 7LB2 glasses and liquids (Figs. 1 and 2, lower curves). These functions allow the separation of the Li environment from the borate network. Although the size of Li is small compared with other alkalis, the structural information obtained from these functions has some general characteristics for all environments of alkalis in borate glasses and melts.

The $\Delta_{Li}(Q)$ and $T_{Li}(r)$ functions are dominated by the Li–O and Li–B pairs (the Li–Li weighting factor is almost negligible). The differential structure factor has oscillations at high Q values ($Q>8$ $Å^{-1}$) because of the Li–O short distances, and exhibits a first negative sharp peak at 1.50 $Å^{-1}$. This latter peak appears at the same position as the first one in the total structure factors, which implies a structural arrangement at medium range involving both the B–O network and the Li environment. The $\Delta_{Li}(Q)$ function makes almost no contribution between 2 and 4 $Å^{-1}$, which indicates a strong anti-phase interference between Li–O and Li–B contributions. In real space, this lack of structural information implies an alternate ordering of Li and B/O atoms that corresponds to a correlation length of ~4.1 Å ($2*\pi/Q$). Such a distance is similar to the distance between (112) planes in crystalline Li–diborate, which suggests that Li atoms may lie between pseudoborate planes.[27] Apart from a

Table II. Gaussian Parameters Used to Fit the B–O Peak in the Total Correlation Functions

Glass	$R_1\pm0.01$ Å	$CN_1\pm0.07$	$\sigma_1\pm0.01$ Å	$R_2\pm0.01$ Å	$CN_2\pm0.07$	$\sigma_2\pm0.01$ Å	N4±0.02
LB2	1.380	1.62	0.060	1.470	1.84	0.096	0.46
NB2	1.380	1.71	0.065	1.485	1.72	0.105	0.43
KB2	1.385	1.8	0.065	1.480	1.60	0.110	0.40
Liquid	$R\pm0.01$ Å	CN±0.12	$\sigma\pm0.01$ Å				N4±0.05
LB2	1.415	3.30	0.115				0.30
NB2	1.420	3.35	0.118				0.35
KB2	1.410	3.32	0.130				0.32

Subscripts 1 and 2 correspond to $^{[3]}$B and $^{[4]}$B in the glassy state, respectively. R is the B–O distance, σ is the Debye–Waller factor, and CN is the coordination number in the liquid state. N4 corresponds to the fraction of $^{[4]}B\backslash(^{[3]}B+^{[4]}B)$.

Table III. Coordination Number, CN_{Li-O}, Debye–Waller Factor, σ_{Li-O}, and Mean Li–O Distance, d_{Li-O}, Obtained by Gaussian Fit of the First Peak in the Li-Centered Differential Correlation Functions $T_{Li}(r)$, Mean Li–B Distances d_{Li-B} and Mean Li–O–B Bond Angles Calculated From the Mean Li–O, Li–B, and B–O Distances Extracted From Neutron Data

T (K)	$d_{Li-O}\pm0.01$ Å	$CN_{Li-O}\pm1.6$	$\sigma_{Li-O}\pm0.01$	$d_{Li-B}\pm0.02$ Å	Li–O–B (deg.)
300	1.995	4.9	0.090	2.95	118
1273	1.97	5.4	0.130	2.99	123

The Gaussian components have been convoluted with the Fourier transform of the Lörch modification function used to calculate the correlation functions.

dampening of the oscillations, the same features are observed in the differential structure factor of the liquid. Therefore, the alternation of Li and B–O is maintained in the melt. The broadening of the first peak indicates that the medium-range arrangements have less extended correlations.

The Li-centered correlation functions, $T_{Li}(r)$, for the glass present a first peak at about 2 Å, ascribed to the Li–O pair,[28] and a second peak at 2.95 Å, assigned mainly to the first Li–B correlation.[20,29] These two peaks are well separated, indicating a well-defined Li polyhedron in the glass. Beyond this range, Li-centered structural oscillations are still observed up to about 12 Å, but their attribution is difficult because of the overlapping of all Li-centered contributions. The first well-defined Li–O peak is maintained in the liquid as well as the two other contributions at about 3 and 4 Å, indicating the persistence of the medium-range ordering around the Li ions. However, drastic changes are observed on increasing the temperature. The first Li–O peak is significantly shifted in position towards the low-r side, and its width is broadened in the liquid. The second peak (Li–B mainly) is shifted by +0.04 Å and becomes narrower and less intense than that in the glass. Similarly, the intensity of the third peak decreases. These differences indicate strong modifications of the mean Li cationic site as the temperature increases. A Gaussian fit of the first Li–O contribution (Table III) confirms a decrease by about 0.02 Å of the mean Li–O distances, while the mean CN is stable (but subject to systematic errors).[29]

(3) Raman Spectra

The evolution of the Raman spectra of LB2 glass with temperature is shown in Fig. 3. In the glass, a strong peak is visible at 770 cm^{-1}, which has been attributed to the localized breathing vibration of six-membered rings containing one or two BO_4 tetrahedra,[5,30] although this band alone cannot be clearly attributed to a particular borate group. The presence of a band at 1130 cm^{-1} indicates the presence of diborate groups, and bands at 520, 670, and 975 cm^{-1} may correspond to tetraborate groups.[30] The prevalence of these groups at diborate compositions has also been observed by NMR studies.[3,4] The high-frequency range is ascribed to stretching of the $B–O^-$ bonds ($O^- = NBO$) attached to large borate groups.[31] Two main bands can be observed in this region at 1410 and 1500 cm^{-1}, which are due to $B\varnothing_2O^-$ triangles ($\varnothing$ = bridging oxygen) linked to $B\varnothing_4^-$ units and $B\varnothing_2O^-$ triangles linked to other BO_3 units.[15] The lower frequency band is thus directly related to the proportion of BO_4 units. These two contributions have been fitted using two Gaussian functions, yielding high- and low-frequency areas denoted as A4 and A3, respectively.

With increasing temperature, the bands present a systematic shift toward lower frequencies because of the thermal expansion. An important decrease in intensities is observed for the bands at medium frequencies (500–1100 cm^{-1}), with almost complete disappearance of the diborate contribution (1100 cm^{-1}). With increasing temperature, we observe drastic changes in the high frequency range (1200–1800 cm^{-1}). The intensity of the lower frequency band decreases relative to that of the high-frequency band. As observed in potassium and sodium diborate glasses,[15,16] the relative area of the two bands A4/A3 does not vary below T_g and decreases above T_g, particularly in the liquid state (Fig. 4). This is thus a direct observation of the conversion of BO_4 units to BO_3 units, which is confirmed by the partial disappearance of the borate rings containing BO_4 units in the medium frequency region. However, the band at 770 cm^{-1} is still present in the liquid state, which could indicate that certain BO_4 units could be preferentially converted while those in ring groups could be stabilized.

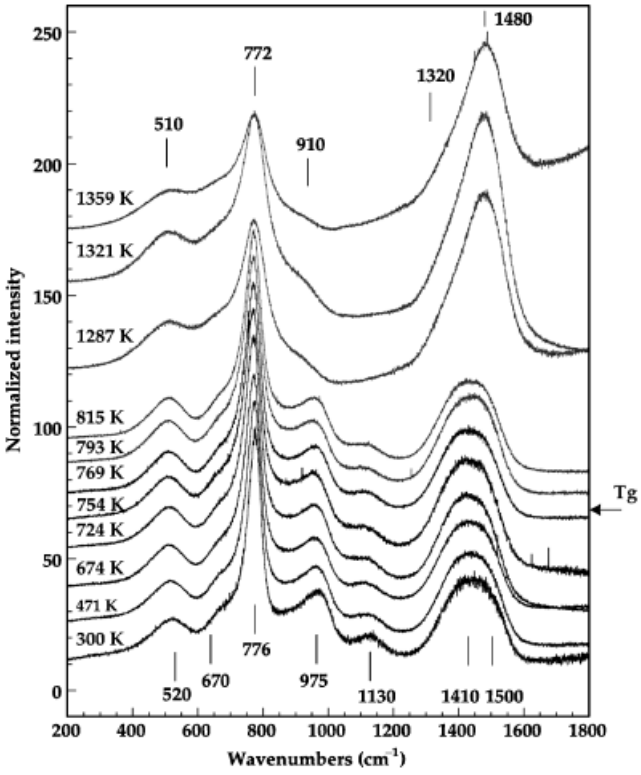

Fig. 3. Raman spectra for the 6LB2 glass from room temperature to 1359 K. The glass transition temperature (T_g) is indicated.

IV. Discussion

(1) Structural Changes Between the Glass and the Melt

(A) Boron and Alkali Environment in Alkali Diborate Glasses: With the neutron data, we observe an increase of N4 as the cation size decreases, which indicates that more NBOs are present in glasses with large alkali cations, in agreement with other methods such as NMR,[4] Raman,[2,32] and infrared reflectance spectroscopies.[2] Such variations have implications toward understanding the structural properties of alkali borate glasses. For instance, it was shown that a greater amount of NBOs decreases the network connectivity of the borate framework, which implies lower T_g and higher thermal expansions.[2,33]

The first difference correlation function, $T_{Li}(r)$, can give information on the structural environment around Li, which may have some generality for other alkalis. In this function, we observe a first peak at 1.995 ± 0.10 Å corresponding to the mean Li–O distance, which suggests that Li is present in an average tetrahedral site.[28] The CN and Debye–Waller factor (σ) for the first Li–O peak are subject to systematic errors that reduce their accuracy.[29] The values obtained for CN (4.9) and σ (0.090 Å) are large, which indicate a distorted Li environment as in Li-aluminosilicate[34] and Li-disilicate glasses.[35] Molecular dynamics simulations on an LB2 glass have also shown that Li sites exist in various distorted environments with four to seven to eight oxygen neighbors.[8] In the LB2 glass, few NBOs are present and mainly BO_4 tetrahedra are formed on introduction of Li_2O.[2,4] Therefore, Li cations mainly have a charge-compensating role

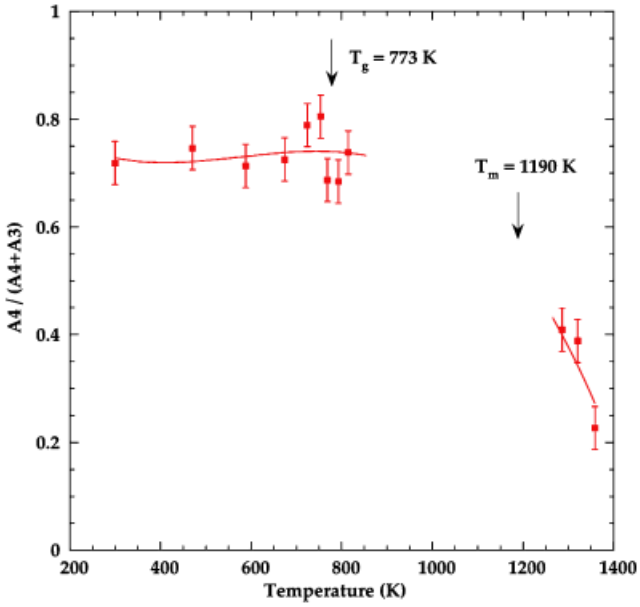

Fig. 4. Ratio of the relative area for the two high-frequency bands of the Raman spectra for the LB2 sample. The temperatures of glass transition and melting are indicated. The line is a guide for the eye.

near the BO_4^- tetrahedra, rather than a modifying role associated with NBOs. These two structural positions have been related to two distinct sites associated with two bands evidenced in the far-IR spectra of alkali borate glasses.[6,7] Recent MD simulations have identified the compensating positions as the largest coordinated sites (seven to eight oxygen neighbors) with a mean Li–O distance of 2.12 Å and no NBO neighbors.[8] This distance is much longer than that observed in our diffraction data with a lower CN, which suggests that the two types of Li sites are less clearly resolved than proposed by MD. A broad Li site distribution is more likely than two well-distinct sites. This is also confirmed experimentally with a close local order around Li in a modifying position in an $Li_2Si_2O_5$ glass or in a charge compensating position in an $LiAlSiO_4$ glass. The main differences reported are with respect to the Li–O distances, which equal 2.02 Å (three O atoms at 1.97 Å and one O atom at 2.20 Å) in the $Li_2Si_2O_5$ glass, and 2.10 Å in $LiAlSiO_4$ glass.[34,35] The Li–B peak is observed at 2.95 Å, which is larger than the Li–B distance of 2.67 Å in the corresponding Li-diborate crystal. This can be explained by a major occurrence of corner sharing between Li-polyhedra and boron units, with a minor occurrence of edge-sharing connections between Li sites and BO_4^- units such as those existing in the crystal.

(B) Structural Changes in the Melt: Both neutron diffraction and Raman data agree with a conversion of the BO_4 tetrahedra to BO_3 triangles above T_g. Because of crystallization, it is difficult to conclude from the Raman spectra as to whether the onset of coordination change starts in the supercooled liquid or in the liquid state. However, Raman data on Na-borate glasses at lower alkali content show that coordination change occurs in the supercooled liquid.[16] An analysis of the first B–O peak gives a direct quantification of this coordination change, with N4 varying from 0.43 in the glass to 0.30 in the liquid. From Raman data on LB2, a quantitative evaluation is more delicate because the band areas are not directly related to the proportion of each species. However, the change in the relative abundance of the high-frequency bands and the disappearance of bands in the mid-frequency region associated with borate rings containing BO_4 tetrahedra are consistent with a change in boron coordination in the liquid state. Similar changes in Raman spectra have also been observed for NB2 and KB2 systems.[15,16] *In situ* ^{11}B NMR measurements yield less accurate values because of averaging of the two isotropical shifts in the liquid.[36]

Modifications at medium-range distances can also be determined in our experimental data. In the total correlation functions, the peak at 2.44 Å is shifted by +0.01 Å and decreases in intensity at high temperature. This peak is dominated by O–O and M–O correlations (M = alkali), with a small contribution from B–B correlations. The significant decrease in intensity can be attributed to the thermal disorder at elevated temperatures and the decrease in the O–O coordination with $^{[4]}B$ to $^{[3]}B$ conversion. Similar to the B_2O_3 melt,[11,12] the shift toward larger r values may be related to larger mean B–O–B angles, resulting from an opening of the borate rings. This agrees with our Raman spectra, which show a decrease of the mid-frequency bands associated with various borate rings containing BO_4 units.

A consequence of the $^{[4]}B$ to $^{[3]}B$ conversion is the formation of NBOs above T_g, which thus depolymerize the borate network and affect the melt properties. Isothermal viscosities at low temperatures are maximum near 25 mol% of alkali oxide in borate melts,[37] which is close to the maximum of formation of BO_4 tetrahedra and thus to a highest connectivity of the network. At higher temperature, the disruption of the network associated with the formation of NBOs results in the disappearance of the maximum in the viscosity isotherms and their progressive decrease with increasing alkali content.

The formation of NBOs also affects the alkali environment, which is clearly seen in the first difference function determined for Li. Indeed, the $T_{Li}(r)$ shows a shift of the Li–O distance from 1.995 Å in the glass to 1.97 Å in the melt. At 1300 K, an increase of the Li–O distances by $\sim$0.02 Å is expected because of the thermal expansion of the Li–O bonds (the mean linear expansion coefficient of Li–O tetrahedra is about 16×10^{-6} K^{-1}).[26] On the contrary, the significant shortening of the Li–O distances is evidence of an important proportion of short Li–O bonds in the melt that correspond to Li–NBO bonds (e.g., the Li–NBO distance is about 0.14 Å smaller than the Li–BO distance in the $Li_2Si_2O_5$ crystal).[38] The increasing number of NBOs in the melt is thus reflected in the first coordination sphere of Li, which is clear evidence of an increasingly modifying role of the alkalis.

At medium-range distances, the mean Li–B distance increases by about 0.04 Å in the melt, resulting in a greater separation of the Li ions from the B atoms in the melt. Li atoms are connected to the borate units through NBOs in the melt. The Li–(NBO)–B angles are likely to be larger than the Li–(BO)–B angles, because NBOs are linked with two atoms (1 B+1 Li), while BOs are linked with three atoms (2 B+1 Li). Because of simple steric hindrance, the mean Li–O–B angle is thus expected to be larger in the melt (Table III), which implies a larger Li–B mean distance. Furthermore, the Li–B peak presents significant decrease in intensity and an apparent narrowing, contrary to a broadening expected by a thermal disordering. These changes are again in agreement with less Li–B connections and, thus, less Li-polyhedra connected to the borate network in the melt than in the glass.

(2) Relationship Between Structural Changes and Properties

(A) Relation to Melt Fragility: Alkali borates are fragile melts whose configurational entropy rapidly decreases at T_g contrary to strong melts such as B_2O_3.[33] In alkali borate melts, the source of configurational entropy lies in the modifications of the boron coordination and the alkali environment, which can be written as

$$BO_4 + Li^{comp} \Leftrightarrow BO_3 + NBO + Li^{mod} \quad (1)$$

where Li^{comp} and Li^{mod} refer to the compensating and modifying positions for Li.

The two structural modifications of the borate network at high temperature, $^{[4]}B$ to $^{[3]}B$ conversion, and rupture of the borate rings involve the breaking of a B–O bond, which yields similar values of enthalpy change, ΔH: 13–37 kJ/mol for the equilibrium reaction (1),[19] and 27 kJ/mol for rearrangement of

the borate rings.[39] Another thermodynamic value of interest is the heat capacity, because the variation of the heat capacity above T_g is ascribed to configurational changes.[1] Similar values are found for the mean change in the heat capacity associated with the boron coordination conversion ($\Delta C_p = \Delta H/(T_1 - T_2) = 75\ J\cdot(mol\cdot K)^{-1}$ for LB2) and the calorimetric difference in C_p ($71\ J\cdot(mol\cdot K)^{-1}$ for LB2).[40] Therefore, the $^{[4]}B$ to $^{[3]}B$ conversion corresponds to the main source of configurational changes in alkali borate systems. A similar conclusion has been deduced from an *in situ* ^{11}B NMR study on alkali borate glasses.[36]

A greater difference in the heat capacity difference, ΔC_p, can be found for KB2:27 and $42\ J\cdot(mol\cdot K)^{-1}$ from the neutron data and calorimetric measurements, respectively.[19] This indicates that other structural changes, possibly at the medium-range distance, may provide a significant contribution to the heat capacity jump at T_g. Indeed, K-borate glasses are known to have a higher amount of NBOs than Li borate glasses and thus less BO_4 tetrahedra to convert.[2] Furthermore, Raman spectra of KB2[15] show the appearance of new bands in the liquid state, contrary to NB2[16] and LB2 (present study). These bands close to 900 and 1100 cm^{-1} could be associated with borate groups containing NBOs, and could thus be an indication of a high amount of NBOs in potassium borate melts. More NBOs will favor the disruption of the network and the flowing of large borate arrangements, which imply structural modifications at medium-range distances.

On the contrary, in pure B_2O_3, a rearrangement of the borate network with no boron coordination change has been observed in the liquid state,[11–13] which yields a small amount of configurational entropy. This agrees with the strong character of the B_2O_3 melt compared with alkali borate melts. Similarly, alkali silicates are stronger melts than alkali borates, because temperature-induced structural changes are less important and reside mainly at medium-range distances.[41]

(B) Alkali Environment and Ionic Diffusion: The environment around alkalis is significantly changed when the temperature increases, as evidenced in the case of Li. Such structural changes can have important consequences on the mobility of ions, as alkali diffusion is a thermally activated process. Indeed, the number of mobile ions in borate glasses has been shown to increase from glassy to liquid state.[42] In borate melts, alkali are increasingly found in modifying positions, which should progressively favor the ionic migration. This is confirmed by MD simulations that have shown that Li mobility increases with the presence of NBOs in the local Li site of various oxide glasses.[8,43–45] This suggests a relationship between the enhanced mobility of Li ions in the melt and NBOs, which could be the existence of regions enriched in alkalis and NBOs. Alkali cations move via hopping through these preferential diffusive pathways.[46,47] Such spatial segregation of Li and NBOs has been evidenced in Li borate glasses and melts by MD simulations.[8] The Li–diborate glass contains few NBOs, and neutron diffraction data are not able to detect whether these NBOs are segregated around Li ions. The situation is different in the melt, which contains more NBOs than in the glass. Our neutron diffraction data give strong support for an association between Li and NBOs by considering the shortening of the mean Li–O distances in the melt. Moreover, the evolution of the second peak in $T_{Li}(r)$ is explained by fewer connections between Li and the borate network in the melt than in the glass, which is indirect evidence for a segregation of Li cations. An understanding of the melt properties thus requires a detailed characterization of the alkali environments at high temperatures and structural modifications between glasses and melts.[41]

V. Conclusions

The proportion of boron in tetrahedral sites, N4, has been shown to decrease between the glass and the liquid in alkali diborate glasses. This coordination change is associated with the formation of NBOs. High-temperature Raman investigation makes it possible to deduce the variation in N4 independently, in excellent agreement with neutron diffraction results. Raman spectra show the disappearance of the associated borate groups containing BO_4 tetrahedra with increasing temperature. The alkali environment is affected by these changes, which was evaluated in the case of Li by using neutron diffraction associated with isotopic substitution of Li. A modification of the structural role is observed: Li is associated with BO_4 tetrahedra in a charge-compensating site in glasses and with NBOs in a modifying position in liquids. The boron coordination change accounts for the main part of the configurational changes and is thus responsible for the fragile character of alkali borate melts. This suggests that structural reorganizations with temperature are related to the dynamic processes above T_g. The modification around alkali environments, in particular, the increasing contribution of NBOs in the first coordination shell in the liquid state, contributes to the increase in the ionic mobility.

Acknowledgments

We are grateful to B. Beuneu and J. P. Ambroise for their help during data acquisition on 7C2 at the L.L.B. and to A. K. Soper for the data acquisition on SANDALS at ISIS.

References

[1]P. Richet and D. R. Neuville, "Thermodynamics of Silicate Melts: Configurational Properties"; pp. 132–60 in *Thermodynamic Data. Systematics and Estimation, Advances in Physical Geochemistry*, Edited by S. Saxena. Springer-Verlag, New York, 1992.

[2]G. D. Chryssikos, E. I. Kamitsos, and M. A. Karakassides, "Structure of Borate Glasses. Part 2. Alkali Induced Network Modifications in Terms of Structure and Properties," *Phys. Chem. Glasses*, **31**, 109–16 (1990).

[3]P. J. Bray, "NMR Studies of the Structure of Glasses," *J. Non-Cryst. Solids*, **95 96**, 45–60 (1987).

[4]J. Zhong and P. J. Bray, "Change in Boron Coordination in Alkali Borate Glasses, and Mixed Alkali Effects, as Elucidated by NMR," *J. Non-Cryst. Solids*, **111**, 67–76 (1989).

[5]W. L. Konijnendijk and J. M. Stevels, "The Structure of Borate Glasses Studied by Raman Scattering," *J. Non-Cryst. Solids*, **18**, 307–31 (1975).

[6]E. I. Kamitsos, M. A. Karakassides, and G. D. Chryssikos, "Cation–Network Interactions in Binary Alkali Metal Borate Glasses. A Far-Infrared Study," *J. Phys. Chem.*, **91**, 5807–13 (1987).

[7]E. I. Kamitsos, A. P. Patsis, and G. D. Chryssikos, "Infrared Reflectance Investigation of Alkali Diborate Glasses," *J. Non-Cryst. Solids*, **152**, 246–57 (1993).

[8]C.-P. E. Varsamis, A. Vegiri, and E. I. Kamitsos, "Molecular Dynamics Investigation of Lithium Borate Glases: Local Structure and Ion Dynamics," *Phys. Rev. B*, **65**, 104203 (2002).

[9]T. Uchino and T. Yoko, "Vibrations of Alkali Cations in Borate Glasses from Molecular Orbital Calculations," *Solid State Ionics*, **105**, 91–6 (1998).

[10]R. J. Elliott, L. Perondi, and R. A. Barrio, "Ionic Conduction in $(1-x)B_2O_3+xLi_2O$," *J. Non-Cryst. Solids*, **168**, 167–78 (1994).

[11]M. Misawa, "Structure of Vitreous and Molten B_2O_3 Measured by Pulsed Neutron Total Scattering," *J. Non-Cryst. Solids*, **122**, 33–40 (1990).

[12]J. Sakowski and G. Herms, "The Structure of Vitreous and Molten B_2O_3," *J. Non-Cryst. Solids*, **293–295**, 304–11 (2001).

[13]A. K. Hassan, L. M. Torell, and L. Börjesson, "Structural Changes of B_2O_3 Through the Liquid–Glass Transition Range: A Raman-Scattering Study," *Phys. Rev. B*, **45**, 12797–805 (1992).

[14]S. Sen, Z. Xu, and J. F. Stebbins, "Temperature Dependent Structural Changes in Borate, Borosilicate and Boroaluminate Liquids: High-Resolution ^{11}B, ^{29}Si and ^{27}Al NMR Studies," *J. Non-Cryst. Solids*, **226**, 29–40 (1998).

[15]R. Akagi, N. Ohtori, and N. Umesaki, "Raman Spectra of K_2O–B_2O_3 Glasses and Melts," *J. Non-Cryst. Solids*, **293–295**, 471–6 (2001).

[16]T. Yano, N. Kunimine, S. Shibata, and M. Yamane, "Structural Investigation of Sodium Borate Glasses and Melts by Raman Spectroscopy. I. Quantitative Evaluation of Structural Units," *J. Non-Cryst. Solids*, **321**, 137–46; 147–156 (2003).

[17]G. Herms and J. Sakowski, "X-Ray Diffraction Studies of Structural Changes in Molten Borate Glasses," *Phys. Chem. Glasses*, **41**, 309–12 (2000).

[18]K. Handa, Y. Kita, S. Kohara, K. Suzuya, T. Fukunaga, M. Misawa, T. Iida, H. Iwasaki, and N. Umesaki, "Structure of M_2O–B_2O_3 (M: Na and K) Glasses and Melts by Neutron Diffraction," *J. Phys. Chem. Solids*, **60**, 1465–71 (1999).

[19]O. Majérus, L. Cormier, G. Calas, and B. Beuneu, "Temperature-Induced Boron Coordination Change in Alkali Borate Glasses and Melts," *Phys. Rev. B*, **67**, 24210 (2003).

[20]O. Majérus, L. Cormier, G. Calas, and B. Beuneu, "Modification of the Structural Role of Lithium Between Lithium-Diborate Glasses and Melts: Implications for Transport Properties and Melt Fragility," *J. Phys. Chem. B*, **107**, 13044–50 (2003).

[21]S. A. Feller, J. Kottke, J. Welter, S. Nijhawan, R. Boekenhauer, H. Zhang, D. Feil, C. Parameswar, K. Budhwani, M. Affatigato, A. Bhatnagar, G. Bhasin, S. Bhowmik, J. Mackenzie, M. Royle, S. Kambeyanda, P. Pandikuthira, and M. Sharma, "Physical Properties of Alkali Borosilicate Glasses"; pp. 246–53 in *Borate Glasses, Crystal and Melts*, Edited by A. C. Wright, S. A. Feller, and A. C. Hannon. The Society of Glass Technology, Sheffield, 1997.

[22]P. Andonov, P. Chieux, and S. Kimura, "A Local Order Study of Molten $LiNbO_3$ by Neutron Diffraction," *J. Phys.: Condens. Matter*, **5**, 4865–76 (1993).

[23]L. Cormier, G. Calas, and P. H. Gaskell, "Cationic Environment in Silicate Glasses Studied by Neutron Diffraction with Isotopic Substitution," *Chem. Geol.*, **174**, 349–63 (2001).

[24]D. A. Long, *Raman Spectroscopy*. McGraw-Hill, New York, 1977.

[25]D. R. Neuville and B. O. Mysen, "Role of Aluminium in the Silicate Network: In Situ, High-Temperature Study of Glasses and Melts on the Join SiO_2–$NaAlO_2$," *Geochim. Comoschim. Acta*, **66**, 1727–37 (1996).

[26]G. E. Brown Jr., F. Farges, and G. Calas, "X-Ray Scattering and X-Ray Spectroscopy Studies of Silicate Melts"; pp. 317–410 in *Structure, Dynamics, and Properties of Silicate Melts, Reviews in Mineralogy*, Vol. 32, Edited by J. F. Stebbins, D. Dingwell, and P. McMillan. Mineralogical Society of America, Washington, DC, 1995.

[27]P. H. Gaskell and D. J. Wallis, "Medium Range Order in Silica, the Canonical Network Glass," *Phys. Rev. Lett.*, **76**, 66–9 (1996).

[28]J. Swenson, L. Börjesson, and W. S. Howells, "Structure of Borate Glasses from Neutron-Diffraction Experiments," *Phys. Rev. B*, **52**, 9310–9 (1995).

[29]O. Majérus, L. Cormier, G. Calas, and A. K. Soper, "The Lithium Environment in Lithium Diborate Glass Studied by Neutron Diffraction with Isotopic Substitution of Li," *Physica B*, **350**, 258–61 (2004).

[30]B. N. Meera and J. Ramakrishna, "Raman Spectra Studies of Borate Glasses," *J. Non-Cryst. Solids*, **159**, 1–21 (1993).

[31]G. D. Chryssikos, E. I. Kamitsos, A. P. Patsis, M. S. Bitsis, and M. A. Karakassides, "The Devitrification of Lithium Metaborate: Polymorphism and Glass Formation," *J. Non-Cryst. Solids*, **126**, 42–51 (1990).

[32]J. Lörosch, M. Couzi, J. Pelous, R. Vacher, and A. Levasseur, "Brillouin and Raman Scattering Study of Borate Glasses," *J. Non-Cryst. Solids*, **69**, 1–25 (1984).

[33]G. D. Chryssikos, E. I. Kamitsos, and Y. D. Yainnopoulos, "Towards a Structural Interpretation of Fragility and Decoupling Trends in Borate Systems," *J. Non-Cryst. Solids*, **196**, 244–8 (1996).

[34]L. Cormier, P. H. Gaskell, G. Calas, J. Zhao, and A. K. Soper, "The Environment Around Li in the $LiAlSiO_4$ Ionic Conductor Glass: A Neutron Scattering and Reverse Monte Carlo Study," *Phys. Rev. B*, **57**, R8067–70 (1998).

[35]J. Zhao, P. H. Gaskell, M. M. Cluckie, and A. K. Soper, "A Neutron Diffraction, Isotopic Substitution Study of the Structure of $Li_2O \cdot 2SiO_2$ Glass," *J. Non-Cryst. Solids*, **234**, 721–7 (1998).

[36]S. Sen, "Temperature Induced Structural Changes and Transport Mechanisms in Borate, Borosilicate and Boroaluminate Liquids: High-Resolution and High-Temperature NMR Results," *J. Non-Cryst. Solids*, **253**, 84–94 (1999).

[37]T. J. M. Visser and J. M. Stevels, "Rheological Properties of Boric Oxide and Alkali Borate Glasses," *J. Non-Cryst. Solids*, **7**, 376–94 (1972).

[38]F. Liebau, "Die Kristallstrukturen Von $Li_2Si_2O_5$, a-$Na_2Si_2O_5$ und $Ag_2Si_2O_5$," *Zum. Naturf.*, **B15**, 467–70 (1960).

[39]R. A. Condrate Sr. and A. K. Jillavenkatesa, "High-Temperature Raman Spectral Studies of Various Borate-Containing Glasses"; pp. 164–72 in *Borate Glasses, Crystals and Melts*, Edited by A. C. Wright, S. A. Feller, and A. H. Hannon. The Society of Glass Technology, Sheffield, 1997.

[40]D. R. Uhlmann, A. G. Kolbeck, and D. L. de Witte, "Heat Capacities and Thermal Behavior of Alkali Borate Glasses," *J. Non-Cryst. Solids*, **5**, 426–43 (1971).

[41]O. Majérus, L. Cormier, G. Calas, and B. Beuneu, "A Neutron Diffraction Study of Temperature-Induced Structural Changes in Potassium Disilicate Glass and Melt," *Chem. Geol.*, **213**, 89–102 (2004).

[42]S. Sen and J. F. Stebbins, "Na-Ion Transport in Borate and Germanate Glasses and Liquids: A ^{23}Na and ^{11}B NMR Spin-Lattice-Relaxation Study," *Phys. Rev. B*, **55**, 3512–9 (1997).

[43]J. Oviedo and J. F. Sanz, "Molecular-Dynamics Simulations of $(Na_2O)_x(SiO_2)_{1-x}$ Glasses: Relation Between Distribution and Diffusive Behavior of Na Atoms," *Phys. Rev. B*, **58**, 9047–53 (1998).

[44]W. Smith, G. N. Greaves, and M. J. Gillan, "The Structure and Dynamics of Sodium Disilicate Glass by Molecular Dynamics Simulation," *J. Non-Cryst. Solids*, **192 and 193**, 267–71 (1995).

[45]A. Karthikeyan, P. Vinatier, A. Levasseur, and K. J. Rao, "The Molecular Dynamics Study of Lithium Ion Conduction in Phosphate Glasses and the Role of Non-Bridging Oxygens," *J. Phys. Chem. B*, **103**, 6185–92 (1999).

[46]G. N. Greaves and K. L. Ngai, "Reconciling Ionic-Transport Properties with Atomic Structure in Oxide Glasses," *Phys. Rev. B*, **52**, 3658–6379 (1995).

[47]P Jund, W. Kob, and R. Julien, "Channel Diffusion of Sodium in a Silicate Glass," *Phys. Rev. B*, **64**, 134303 (2001). □